Arch Microbiol (2015) 197:1129–1139
DOI 10.1007/s00203-015-1153-9

ORIGINAL PAPER

Carotenoid production and gene expression in an astaxanthin-overproducing *Xanthophyllomyces dendrorhous* mutant strain

Lina M. Castelblanco-Matiz[1] · Alejandra Barbachano-Torres[1] · Teresa Ponce-Noyola[1] · Ana C. Ramos-Valdivia[1] · Carlos M. Cerda García-Rojas[2] · César M. Flores-Ortiz[3] · Salvador K. Barahona-Crisóstomo[4] · Marcelo E. Baeza-Cancino[4] · Jennifer Alcaíno-Gorman[4] · Víctor H. Cifuentes-Guzmán[4]

Received: 27 May 2015 / Revised: 7 August 2015 / Accepted: 11 September 2015 / Published online: 16 September 2015

Abstract The primary carotenoid synthesized by *Xanthophyllomyces dendrorhous* is astaxanthin, which is used as a feed additive in aquaculture. Cell growth kinetics and carotenoid production were correlated with the mRNA levels of the *idi*, *crtE*, *crtYB*, *crtI*, *crtS* and *crtR* genes, and the changes in gene sequence between the wild-type and a carotenoid overproducer XR4 mutant strain were identified. At the late stationary phase, the total carotenoid content in XR4 was fivefold higher than that of the wild-type strain. Additionally, the mRNA levels of *crtE* and *crtS* increased during the XR4 growth and were three times higher than the wild-type strain in the late stationary phase. Moreover, the nucleotide sequences of *crtYB*, *crtI* and *crtR* exhibited differences between the strains. Both the higher *crtE* and *crtS* transcript levels and the *crtYB*, *crtI* and *crtR* mutations can, at least in part, act to up-regulate the carotenoid biosynthesis pathway in the XR4 strain.

Keywords Astaxanthin · Carotenoid biosynthesis · Gene expression · Mutations · Overproducer strain · *Xanthophyllomyces dendrorhous*

Introduction

The basidiomycetous yeast *Xanthophyllomyces dendrorhous* (the sexual state of *Phaffia rhodozyma*) forms orange-red colonies due to carotenoid production, and it is the only fungus that synthesizes substantial amounts of astaxanthin (Rodriguez-Saiz et al. 2010). This carotenoid (3,3′-dihydroxy-β-β'-carotene-4,4′-dione) is one of the most important pigments with a high biotechnological interest, primarily in the aquaculture industry, as it is responsible for the orange-red flesh color of salmon and trout (Chimsung et al. 2014). In addition to its applications in coloration, astaxanthin is also recognized for its potent antioxidant properties and other beneficial effects on human health (Ambati et al. 2014).

The carotenoid pathway of *X. dendrorhous* is well established, arising via the mevalonate pathway (Gassel et al. 2014). The genes encoding isopentenyl pyrophosphate isomerase (*idi*), geranylgeranyl pyrophosphate synthase (*crtE*), phytoene synthase–lycopene cyclase (*crtYB*), phytoene desaturase (*crtI*), astaxanthin synthase (*crtS*) and cytochrome P450 reductase (*crtR*) have been characterized and overexpressed (Schmidt et al. 2011). Their expression has been studied in some parental and mutant strains (Lodato et al. 2007; Miao et al. 2011; Wozniak et al. 2011) in different attempts to understand the complex regulatory system of carotenoid biosynthesis in *X. dendrorhous*.

In previous work, an astaxanthin-overproducing *X. dendrorhous* mutant, named XR4, was obtained by Barbachano-Torres et al. (2014). However, no information is

Communicated by Jorge Membrillo-Hernández.

✉ Teresa Ponce-Noyola
tponce@cinvestav.mx

[1] Departamento de Biotecnología y Bioingeniería, CINVESTAV-IPN, Av. Instituto Politécnico Nacional 2508, Zacatenco, 07360 Mexico, D.F., Mexico

[2] Departamento de Química, CINVESTAV-IPN, 07360 Mexico, D.F., Mexico

[3] Facultad de Estudios Superiores Iztacala, UNAM, 54090 Mexico, D.F., Mexico

[4] Centro de Biotecnología y Departamento de Ciencias Ecológicas, Facultad de Ciencias, Universidad de Chile, Las Palmeras 3425, Casilla 653, Santiago, Chile

available for this strain as to the expression of the genes involved in the carotenoid biosynthesis pathway or the changes in the nucleotide sequence of these genes due to the mutagenesis process.

In this work, to identify potential causes of excessive carotenoid and astaxanthin accumulation in the XR4 strain, we compared the expression at the mRNA level of six of the genes controlling carotenoid biosynthesis, from isopentenyl pyrophosphate (IPP) to astaxanthin, and we correlated these data to the carotenoid production during the growth of the wild-type and XR4 mutant strains. In addition, we performed gene sequence analyses in both strains.

Materials and methods

Yeast strains and culture conditions

X. dendrorhous wild-type CDBB-L-685 (ATCC 24202) was obtained from the "Colección Microbiana Departamento de Biotecnología y Bioingeniería," CINVESTAV Mexico, and the XR4 mutant strain generated by *N*-methyl-*N*′-nitro-*N*-nitrosoguanidine (NTG) treatment of the parental strain (Barbachano-Torres et al. 2014). The strains were grown in 1-L Erlenmeyer flasks containing 375 mL YM medium (0.3 % yeast extract, 0.3 % malt extract and 0.5 % peptone) supplemented with 1 % glucose at 22 °C and 160 rpm. The growth curves were constructed to assess yeast cell growth by measuring the optical density (OD) at 600 nm and included the analyses of total carotenoid, carotenoid composition and relative mRNA levels of the six genes involved in the carotenoid pathway at four time points. Samples were taken after 24, 37, 61 and 87 h of cultivation (early exponential, late exponential, stationary and late stationary phases of growth, respectively). All analyses were performed at least in triplicate from three independent cultures, and statistical significance was established using Student's *t* test at a $p \leq 0.05$.

Carotenoid extraction and RP-HPLC

Carotenoids were extracted from cellular pellets by the acetone extraction method (An et al. 1989). Total carotenoids were quantified by absorbance at 474 nm using an absorption coefficient of $A_{1\ \%} = 2100$ and normalized to the dry cell weight (dcw) of the yeast. The carotenoid profile was characterized by RP-HPLC using a reverse phase RP-18 LichroCART125-4 (Merck) column with acetonitrile:methanol:isopropanol (85:10:5 v v^{-1}) as the mobile phase with a 1 mL min^{-1} flux. The elution spectra were recovered using a diode array detector, and carotenoids were identified by their spectra and retention time (Britton et al. 2008).

DNA amplification and sequence analyses

The oligonucleotides designed and used in this study were synthesized by Integrated DNA Technologies (Table 1). In general, PCRs were performed in a final volume of 25 µL containing 2 U of *Taq* DNA polymerase, 2.5 µL of 10X *Taq* buffer, 0.5 µL of 10 mM dNTPs, 1 µL of 50 mM $MgCl_2$, 1 µL of 25 µM of each primer and 10–20 ng of template DNA. The DNA amplification reactions were performed in a thermal cycler 2720 (Applied Biosystems) as follows: initial denaturation at 95 °C for 3 min; 35 cycles of denaturation at 94 °C for 30 s, annealing at 55 °C for 30 s, synthesis at 72 °C for 3 min and a final extension step at 72 °C for 10 min. The samples were kept at 4 °C until analysis. The amplicons were separated by 1.0 % agarose gel electrophoresis in TAE buffer containing 0.5 µg mL^{-1} ethidium bromide (Sambrook and Russell 2001) followed by DNA purification using the glass milk method (Boyle and Lew 1995). The nucleotide sequences of the six genes from both strains were obtained from an ABI 3100 Avant genetic analyzer using the BigDye terminator v3.1 kit (Applied Biosystems) and by DNA sequencing (Macrogen Inc.). DNA sequences were analyzed using Vector NTI Suite 10 (Informax) and programs available at the NCBI Web site. Analysis of promoter region of the carotenogenic genes was performed using the YEASTRACT database (Teixeira et al. 2014).

RNA extraction, single-strand DNA synthesis and RT-qPCR

The cell pellets from 5 mL culture aliquots of each time point were frozen immediately by immersion in ethanol at −80 °C and stored at that temperature until use. Total RNA extraction was performed as described elsewhere (Chomczynski and Sacchi 1987) as modified by Lodato et al. (2004). The cell pellets were suspended in 200 µL of lysis buffer (0.02 M sodium acetate pH 5.5, 0.5 % SDS, 1 mM EDTA) and were broken through mechanical rupture with 0.5 mm glass beads (BioSpec) and shaking in a mini bead beater (BioSpec) for 1 min. Then, 800 µL of Tri-Reagent (Ambion) was added, followed by shaking in the bead beater for 1 min and incubation for 10 min on ice. Next, 200 µL of chloroform was added, followed by mixing and incubation for 6 min at room temperature and centrifugation for 10 min at 14,000*g*. RNA was extracted from the recovered aqueous phase by precipitation with 1 volume of isopropanol and 0.5 volume of precipitation buffer (1.2 M NaCl, 0.8 M sodium citrate) for 1 h at −20 °C. The RNA was washed with 70 % ethanol, suspended in RNase-free H_2O and quantified spectrophotometrically at 260 nm in a V-630 UV–Vis spectrophotometer from JASCO.

The cDNA was synthesized using M-MLV reverse transcriptase (Invitrogen) with 5 µg of total RNA in a final

Table 1 Primers designed and used in this work

No.	Primer name[a]	Sequence	Target
1	idi sec fw1	TCTTGACCAGAGCTAAACCC	Upstream *idi* gene
2	idi sec fw2	GGCGAAAGACGAACTGAACG	Upstream *idi* gene
3	idi sec fw3	GCAGGCCGTTGAAGACTCG	Upstream *idi* gene
4	idi sec fw4	ATTCCTTCTGCGTCGTTTCG	*idi* gene
5	idi sec fw5	TCCTCTTACCTGGTGGTATG	*idi* gene
6	idi sec fw6	AACGAAGTCTCTGACACTCG	*idi* gene
7	idi sec rev7	TGATCTGAAATGTTGTAGCCC	Downstream *idi* gene
8	crtE sec fw1	ACAACAACAAAAGCTTCTGGC	Upstream *crtE* gene
9	crtE sec fw2	ACTGTTCATACATGTCCATCG	Upstream *crtE* gene
10	crtE sec fw3	CCTCACAGCAATTCCACTCG	*crtE* gene
11	crtE sec fw4	TCTTTTCCTCATCCTCTTGCC	*crtE* gene
12	crtE sec fw5	CTGACTTGTCTATTCTGACCG	*crtE* gene
13	crtE sec fw6	GTATTCATCTGACCAGCATTCG	*crtE* gene
14	crtE sec fw7	AGTCTTCTGAGGTACTTATCG	*crtE* gene
15	crtE sec rev8	ATGAGAAGGAAATCAAAGAGGG	Downstream *crtE* gene
16	crtYB sec fw1	ATGGGGAATTCCAGTTTTGCC	Upstream *crtYB* gene
17	crtYB sec fw2	CTTATTGCTCAACTCAGTTGG	Upstream *crtYB* gene
18	crtYB sec fw3	CTTACCCAACTCGTATCATCC	Upstream *crtYB* gene
19	crtYB sec fw4	TGTTCCATATGAAGAGTACGC	*crtYB* gene
20	crtYB sec fw5	GCTATGTTCTTCTTACTGACG	*crtYB* gene
21	crtYB sec fw6	CATAACAGATACGCATTCTGC	*crtYB* gene
22	crtYB sec fw7	CTATTGGTCTATGTCTCTTGG	*crtYB* gene
23	crtYB sec fw8	CGTTTGGAAAGGAGACGTCG	*crtYB* gene
24	crtYB sec rev9	AGAACCAGTTGGCAAGGACG	Downstream *crtYB* gene
25	crtI sec fw1	ACTCATCTCAACATGGCCCG	Upstream *crtI* gene
26	crtI sec fw2	GAGCATAAGCGCCTGTCCG	Upstream *crtI* gene
27	crtI sec fw3	AGATCAGGATAAACCCACAGC	*crtI* gene
28	crtI sec fw4	CTCATCATTCGTCCACAACG	*crtI* gene
29	crtI sec fw5	CACTTCCACGATGTATGTACC	*crtI* gene
30	crtI sec fw6	ACCGACAGATTACGAAGAGTC	*crtI* gene
31	crtI sec fw7	GAAGTCAAGAGAAGTTGGTGG	*crtI* gene
32	crtI sec fw8	TACAACAAGCTTGTTGCTCGG	*crtI* gene
33	crtI sec rev9	TATTGAGCGGGTTTAGATGCG	Downstream *crtI* gene
34	crtS sec fw1	GTCCGGCATCGAAACCTGG	Upstream *crtS* gene
35	crtS sec fw2	TCGCCAGCAGTTGATCAAGC	Upstream *crtS* gene
36	crtS sec fw3	ATACTACCCGTCGATTCTAACC	Upstream *crtS* gene
37	crtS sec fw4	GTACAGATGAAGAGCATGCG	*crtS* gene
38	crtS sec fw5	GACAAGATGATGGAGGATGC	*crtS* gene
39	crtS sec fw6	CCGAACTATGGTATGTCTGC	*crtS* gene
40	crtS sec fw7	AAAGCTGTCCGATGAGGAGG	*crtS* gene
41	crtS sec fw8	CTAACCGTGAATGCTTGAAGG	*crtS* gene
42	crtS sec fw9	CAGACTCGCTCAACAGTATTG	*crtS* gene
43	crtS sec rev10	AGGAGTAAGAACAAGTGGAGG	Downstream *crtS* gene
44	crtR sec fw1	AGCGCTGAAGAGAGGATTCG	Upstream *crtR* gene
45	crtR sec fw2	GCATCACCTATGTGTCTATCG	Upstream *crtR* gene
46	crtR sec fw3	ACTCTCCGATCTTGTCATCC	Upstream *crtR* gene
47	crtR sec fw4	TGTTTTACGGCTCCCAGACG	*crtR* gene
48	crtR sec fw5	GTCGGTAGACAGCTTGACG	*crtR* gene
49	crtR sec fw6	ATCCAGGTTGTCTCGCTCG	*crtR* gene
50	crtR sec fw7	CGGATTGGGCACAAACTACC	*crtR* gene

Table 1 continued

No.	Primer name[a]	Sequence	Target
51	crtR sec fw8	TACGTTCAGGATCTTTTGTGG	*crtR* gene
52	crtR sec rev9	TTCCTCTTGCTTTCTTCGTCG	Downstream *crtR* gene
RT-qPCR			
53	mActF-RT	CCGCCCTCGTGATTGATAAC	*Actin* gene
54	mActR-RT	TCACCAACGTAGGAGTCCTT	*Actin* gene
55	midif-RT	TCCGAACCGAAGGACTCAGTTT	*idi* gene cDNA (for qPCR)
56	midir-RT	GGACATCAAGTGGCAGGTCT	*idi* gene cDNA (for qPCR)
57	mcrtEf-RT	TGTTGGCATGCTACATACCG	*crtE* gene cDNA (for qPCR)
58	mcrtER-RT	GTTGGGCGAAGCTTGAAGAT	*crtE* gene cDNA (for qPCR)
59	mmcrtYBF2-RT	TCGCATATTACCAGATCCATCTGA	*crtYB*(mm) gene cDNA (for qPCR)
60	mmcrtYBR2-RT	GGATATGTCCATGCGCCATT	*crtYB* (mm)gene cDNA (for qPCR)
61	mmcrtIF-RT	CATCGTGGGATGTGGTATCG	*crtI* (mm)gene cDNA (for qPCR)
62	mmcrtIR-RT	GGCCCCTGATCGAATCGATAA	*crtI*(mm) gene cDNA (for qPCR)
63	mcrtSf-RT	ATGGCTCTTGCAGGGTTTGA	*crtS* gene cDNA (for qPCR)
64	mcrtSR-RT	TGCTCCATAAGCTCGATCCCAA	*crtS* gene cDNA (for qPCR)
65	mcrtRf-RT	CTGGGAAACAAGACCTACGA	*crtR* gene cDNA (for qPCR)
66	mcrtRR-RT	GGAACCTCGGTTACGACAAA	*crtR* gene cDNA (for qPCR)

(mm), mature transcript

[a] fw, F and rev, R in the primer name indicate the primer orientation

volume of 20 µL, according to the manufacturer's protocol. The relative transcript level analyses for each gene were performed in an Mx3000P quantitative PCR system (Stratagene) using 1 µL of the reverse transcription reaction and 10 µL of the SensiMix SYBR Hi-ROX kit (Bioline) in a final volume of 20 µL. The C_T values were normalized to the respective value of the *X. dendrorhous* actin gene [Genbank: X89898.1] (Lodato et al. 2007) and were later expressed as a function of the control conditions using the $\Delta\Delta C_T$ algorithm (Schmittgen and Livak 2008).

The nucleotide sequences were registered in the GenBank database under the following accession numbers: wild-type *idi* [KR779659], XR4 *idi* [KR779660] wild-type *crtE* [KR779661], XR4 *crtE* [KR779662], wild-type *crtYB* [KR779663], XR4 *crtYB* [KR779664], wild-type *crtI* [KR779665], XR4 *crtI* [KR779666], wild-type *crtS* [KR779667], XR4 *crtS* [KR779668] and wild-type *crtR* [KR779669], XR4 *crtR* [KR779670].

Results and discussion

Growth and carotenoid production

With the aim of characterizing carotenoid production during the growth of *X. dendrorhous* wild-type and its XR4 mutant strains, the strains were grown in batch cultivation until 87 h. The exponential growth phase was similar in both cultures, beginning after 15 h of lag phase (Fig. 1). The mutant XR4 strain had slightly lower cell growth values during the exponential phase (Student's t test, $p \leq 0.05$). However, during the stationary phase, similar OD values were reached by both strains. Similar behavior was observed in *X. dendrorhous* wild-type UCD 67-385 and its carotenoid-overproducing mutants 385-*cyp61*$^{(+/-)}$ and 385-*cyp61*$^{(-/-)}$ growing in the same medium used in this study (Loto et al. 2012). This range of values has also been reported in other *X. dendrorhous* strains obtained by random mutagenesis (Schmidt et al. 2011) due to a possible carbon flux redirection in their carotenoid biosynthesis pathway (Lodato et al. 2007).

Carotenoids were extracted and quantified from cell pellets after 24, 37, 61 and 87 h of cultivation (early exponential, late exponential, stationary and late stationary phases of growth, respectively). An accumulation of total carotenoid content was observed in both strains throughout the growth phases (Fig. 1).

By the naked eye, a different pigmentation phenotype between the wild-type and its mutant strain was observable, where the mutant had a more intense red color, suggesting a higher carotenoid production. This was quantitatively confirmed; the XR4 strain produced more carotenoids than the wild-type strain at all phases of growth. In both strains, the total carotenoid content increased along the growth

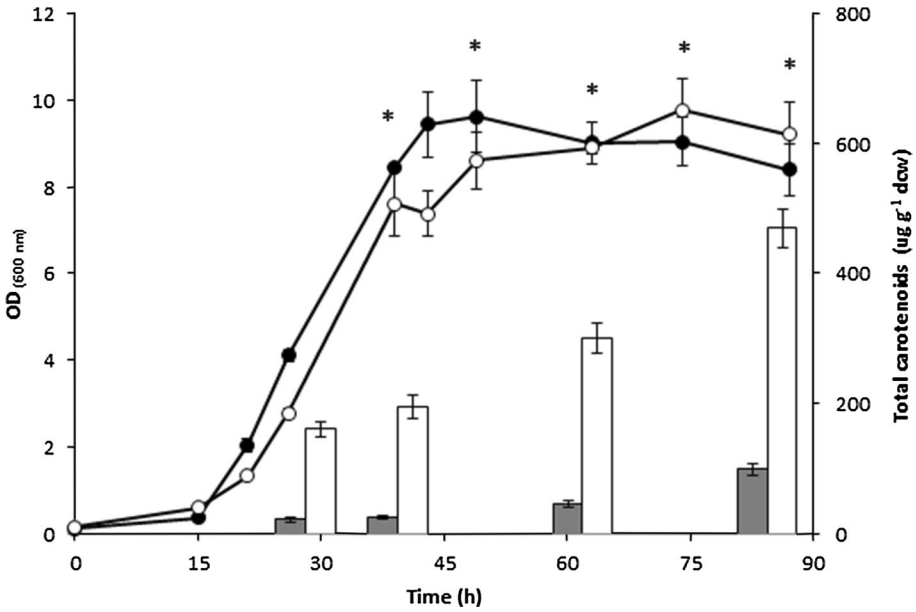

Fig. 1 Growth curve and total carotenoid production after 24, 37, 61 and 87 h of cultivation of the wild-type (*black circles* and *gray bars*) and XR4 mutant (*white circles* and *bars*) *X. dendrorhous* strains. The values are the mean of three independent experiments, and the *error bars* correspond to the standard deviations (*asterisks* indicate values with $p > 0.05$; Student's *t* test)

curve, reaching the maximum carotenoid content at the late stationary phase. At this phase, the XR4 strain had a 4.7-fold higher total carotenoid content compared to the wild-type strain, reaching 470.1 μg g^{-1} dcw total carotenoid in contrast to the wild type, which only reached 99.2 μg g^{-1} dcw (Fig. 1).

A slight increase in the total carotenoid production from the early exponential to the late exponential phases was observed in the wild-type and XR4 strains; however, the main carotenoid accumulation in both strain cultures occurred during the stationary phase and continued increasing until 87 h of culture. This finding indicates that carotenoid production is associated with the age and the lower growth rate of the culture, which is in agreement with previous results (Lodato et al. 2007; Gassel et al. 2013).

Carotenoid synthesis could be induced approximately at the end of the exponential phase and during the stationary phase by some reactive oxygen species, which are naturally present in cells as by-products of oxidative metabolism that can increase with time as a function of culture age (Schroeder and Johnson 1995). At this stage, catabolism together with a low energy demand should increase the NADH/NAD+ ratio in the cells, inhibiting TCA cycle activity by an excess of energy and providing a surplus of carbon skeletons for isoprenoid biosynthesis by the mevalonate pathway (Chávez-Cabrera et al. 2010). This could cause an increase in *X. dendrorhous* pigment production. Moreover, Marcoleta et al. (2011) suggested that there is another possible mechanism underlying increased pigmentation production, which involves changes at the mRNA level of several genes. The authors explained, at least in part, the induction of carotenoid production in the wild-type *X. dendrorhous* strain UCD67-385 by a significant increase in the mRNA levels of two of the three genes required for the synthesis of astaxanthin from geranylgeranyl pyrophosphate (GGPP). These data support the importance of the regulation of gene expression at the transcriptional level in the regulation of this pathway.

The carotenoid composition at each growth phase was also analyzed. An increased proportion of astaxanthin relative to the total carotenoid content was observed in both strains. In the wild-type strain, the percentage of astaxanthin in relation to the other carotenoids decreased from 76.1 % at the late exponential phase to 44.5 % at the late stationary phase, indicating the generation or accumulation of carotenoid intermediates such as phoenicoxanthin, canthaxanthin, OH-ketotorulene, keto-γ-carotene, echinenone and β-carotene (Table 2). In the XR4 strain, the amount of astaxanthin remained relatively constant at approximately 85 % over all the growth phases, which can be explained by a faster conversion of most of the intermediates to the final product of the pathway. An increase in almost eightfold in the amount of astaxanthin was present at the late stationary phase in the XR4 strain compared to the wild type.

Sequence analysis of genes encoding for carotenoid biosynthesis

The mutagenic process in the *X. dendrorhous* XR4 strain could generate different mutations in the structural genes involved in the carotenogenic process, which could explain the differences in phenotype between the wild-type and XR4 mutant strains. The complete ORF sequence and approximately 1.0 Kb upstream of each ORF of the six structural carotenogenic genes studied were obtained and compared among the strains. All of the XR4 genes

Table 2 Carotenoid composition of the wild-type and XR4 *X. dendrorhous* mutant strains

Cultivation time (h)/carotenoids (μg g^{-1} dcw)	Wild type				XR4			
	24	37	61	87	24	37	61	87
X. dendrorhous strains								
Astaxanthin	17.2	19.7	28.4	45.9	134.0	223.4	249.2	403.9
Phoenicoxanthin	1.8	3.1	4.6	9.2	11.3	10.0	31.9	46.4
Canthaxanthin	ND	ND	ND	1.3	ND	ND	ND	ND
OH-ketotorulene	1.9	3.2	3.8	9.7	11.3	10.4	16.6	18.9
Keto-γ-carotene	0.3	ND	2.3	7.0	2.3	ND	ND	5.8
Echinenone	ND	ND	ND	6.9	1.3	ND	ND	ND
β-carotene	0.7	ND	8.9	28.8	2.2	ND	22.8	6.2
Total carotenoids	21.2	24.8	46.0	99.2	160.3	195.9	300.4	470.1

The values are the mean of three independent experiments. Standard deviations (not shown) were lower than 10 %

ND Not detected

Table 3 Mutations in genes encoding for carotenoid biosynthesis in *X. dendrorhous* wild-type and XR4 strains

Gene	Nucleotide changes	Upstream region	Exonic region	Intronic region	Amino acid change
idi	1	–	–	1	–
crtE	1	–	1	–	–
crtYB	1	1	–	–	–
crtI	3	–	2	1	Q^{5}–K H^{427}–Q
crtS	9	–	1	8	–
crtR	122	60	40	22	T^{111} insertion Y^{156}–D N^{521}–T

exhibited at least one nucleotide change; however, only *crtI* and *crtR* showed missense mutations, causing H to Q and Y to D amino acid changes, respectively. This type of change could partially explain the different patterns of carotenoids produced among the strains. On the other hand, only *crtYB* and *crtR* contained mutations in their upstream region (Table 3). Several common regulatory elements (*cis* acting elements) have been reported in the corresponding promoter regions of these genes, like the Mig1 (MADS-box transcription factor Mig1) binding sequence described in the upstream region of the *crtYB* gene (Wozniak et al. 2011) and in several glucose-repressed genes. Mig1 binds to the regulatory sequences and specifically blocks the transcription of these genes in the presence of glucose (Rolland et al. 2002). Similar sequences generated or modified throughout the mutagenic process in the promoter region of *crtYB* and *crtR* genes could be affecting the regulation of their expression, leading to a carotenoid-overproducing phenotype. Thus, the mRNA levels of the genes *idi*, *crtE*, *crtYB*, *crtI*, *crtS* and *crtR* were evaluated in both strains at the different time points of the growth curve.

Expression of the genes involved in the carotenoid pathway

Using RT-qPCR analysis, the relative expression values were normalized to the housekeeping actin gene and were later expressed as a function of the wild-type values, whose carotenogenic transcript levels were defined as one (Schmittgen and Livak 2008; Marcoleta et al. 2011). The gene expression pattern at the mRNA level between XR4 and its parental strain was different for most of the analyzed genes (Fig. 2).

The expression of the *X. dendrorhous* XR4 *idi* gene did not have a clear pattern throughout the growth cycle (Fig. 2a). The lowest value was observed at the stationary phase while the total carotenoid content increased, and no significant differences between the strains were observed at the end of the stationary phase (Student's *t* test, $p \geq 0.05$). A decrease in XR4 *idi* mRNA level during the stationary phase has also been reported in other carotenoid-overproducing *X. dendrorhous* mutant strains, suggesting that an increase in *idi* gene expression was not associated with an increase in carotenoid production (Lodato et al. 2007).

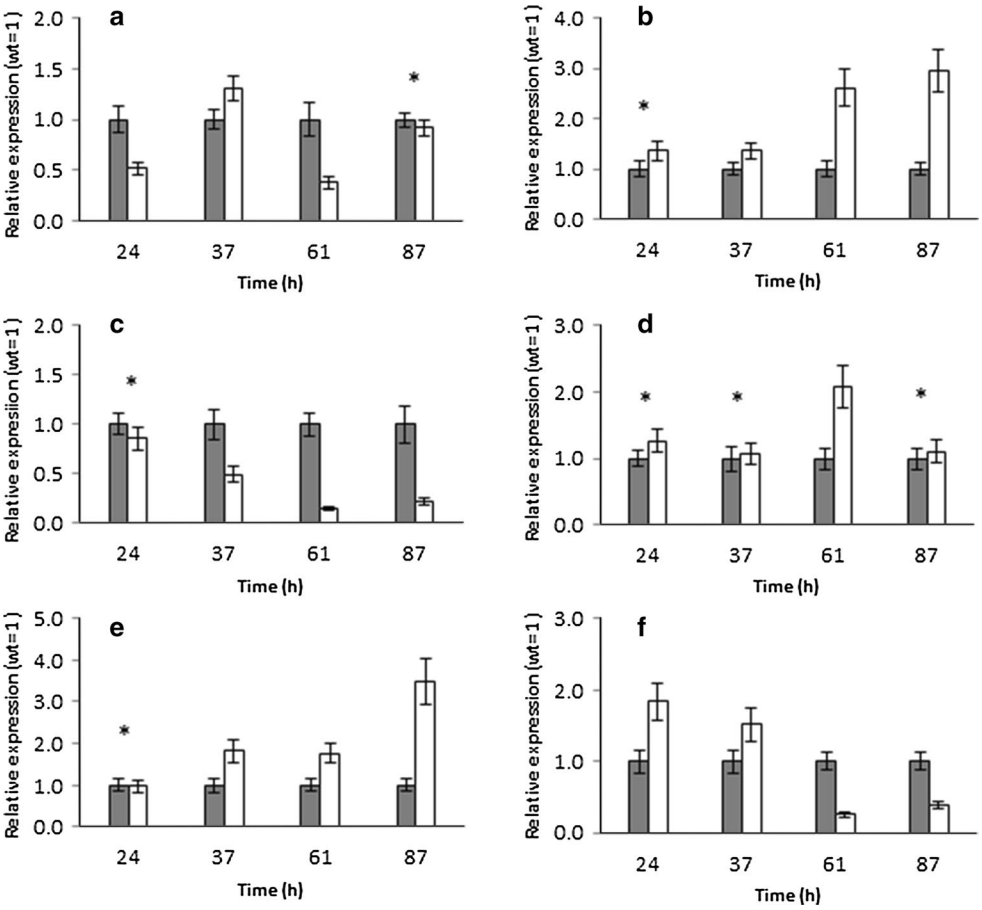

Fig. 2 RT-qPCR analysis of *X. dendrorhous* carotenogenic structural genes in the wild-type and XR4 strains. The **a** *idi*; **b** *crtE*; **c** *crtYB*; **d** *crtI*; **e** *crtS*; and **f** *crtR* transcript levels were determined by RT-qPCR after 24, 37, 61 and 87 h of cultivation. Each transcript level was normalized with respect to the transcript level of the actin gene and then to the wild-type strain (=1, *gray bars*). The values are the mean of three independent experiments, and the *error bars* correspond to the standard deviations (*asterisks* indicate values with $p \geq 0.05$; Student's *t* test)

Miao et al. (2011) did not find obvious differences in the transcript levels of genes involved in the mevalonate pathway, such as *idi*, *MVK* and *MPD*, or other genes, such as *FPS*, responsible for the early steps of astaxanthin biosynthesis in *X. dendrorhous*, between the carotenoid-overproducing MK19 mutant strain and the JCM9042 wild-type strain. Although in a recombinant *E. coli* strain IPP isomerase was a limiting enzyme for carotenoid synthesis because *idi* overexpression increased carotenoid production, its overexpression in *X. dendrorhous* decreased the astaxanthin content and total carotenoid production (Visser et al. 2005). This result suggests the existence of next appearing limiting steps in the *X. dendrorhous* carotenoid biosynthesis pathway.

The *crtE* gene expression in the XR4 strain was higher than in the wild-type strain along the growth curve (Fig. 2b). The mutant strain showed a constant increase in the *crtE* mRNA level from the late exponential phase to the late stationary phase, coinciding with carotenoid production. At the end of the *crtE* gene expression kinetics analysis, the XR4 was almost threefold higher compared to the parental strain. The *crtE* gene controls the formation of GGPP, which is the first step of carotenoid synthesis. Thus, its higher level in the XR4 strain could explain, at least in part, the higher carotenoid level in the mutant strain: 4.7-fold higher than in the wild-type strain. This result is in agreement with previous reports, where *crtE* gene overexpression in the CBS6938 *X. dendrorhous* strain diverted the metabolite flow from the sterol pathway toward carotenoid biosynthesis, leading to transformants with higher carotenoid levels (Breitenbach et al. 2011).

The *crtYB* gene expression was similar in both strains at the early exponential growth phase. However, a decrease in *crtYB* mRNA level in XR4 was observed throughout the yeast growth cycle, even when the main carotenoid production occurred (Fig. 2c). Thus, similar to *idi*, *crtYB* gene expression should not be associated with carotenoid accumulation in the XR4 strain, which is notably different from other studies. The introduction of extra copies of the *crtYB* gene resulted in transformants with a higher total carotenoid content, primarily β-carotene and ketocarotenoid intermediates (produced by the phytoene synthase activity) and with a strong decrease in 3-HO-4-ketotorulene (HKT), the alternative product of *X. dendrorhous* carotenoid biosynthesis (by lycopene cyclase activity; Verdoes et al. 2003). Although no changes were found in the XR4 *crtYB* ORF sequence, the particular decrease in its gene expression could be due to the A–G transition found

in the promoter region resulting in the sequence CTCGA (524–528 nucleotides upstream of the translation initiation site; Table 3). The CTCGA sequence, whose expression is induced by stress or starvation during mitosis and late in meiosis, was previously reported as a binding site for the Xbp1p transcription factor (Rintala et al. 2009). Due to Xbp1p is a transcriptional repressor, its binding to the CTCGA sequence could be responsible for the decrease in the XR4 *crtYB* mRNA level.

The mRNA expression kinetics of *crtI* in the wild-type and XR4 strains was similar during the exponential growth phase (Fig. 2d). A twofold increase in the XR4 *crtI* transcript level was observed at the stationary phase, while the production of carotenoids was increasing; however, no significant differences from the wild-type strain were detected at the end of the culture when carotenoids were still accumulating (Student's t test, $p \geq 0.05$). This result suggests that in the XR4 strain, *crtI* gene expression kinetics is not directly associated with the increased carotenoid production. It has been reported that when *crtI* is overexpressed, the formation of monocyclic carotenoids such as torulene and HKT is higher because of a higher desaturase activity, whereas the content of bicyclic carotenoids such as echinenone and β-carotene decrease, including a 50 % astaxanthin reduction (Visser et al. 2003). Thus, the decrease in the XR4 *crtI* mRNA level at the end of the culture may partially explain its high astaxanthin ratio. The XR4 *crtI* sequence analysis revealed the replacement of residue Q to K at position 5 (due to a C to A transversion in nucleotide 13, exon 1) and of H to Q at position 427 (due to a C to A transversion in nucleotide 1281, exon 12; Table 3). These mutations may contribute to the phenotype of the mutant strain, as the first mutation is located in a loop upstream of the [NAD(H)/NADP(H)/FAD(H)]-binding domain (Verdoes et al. 1999). Although a Q to K amino acid substitution is rarely involved directly in protein function, the large and flexible side chain in lysine frequently plays an important role in protein structure (Betts and Russell 2007) and could be involved in XR4 protein stability. The second mutation is located in an α-helix upstream of the carotenoid-binding domain (Verdoes et al. 1999), and as H and Q amino acids are quite frequently involved in protein-active or protein-binding sites (Betts and Russell 2007), this substitution also may play a role in protein complex formation or protein stability. Thus, these missense mutations in the XR4 strain could explain, at least in part, the lack of a relation between mRNA levels and carotenoid accumulation during the stationary growth phase.

In *X. dendrorhous*, astaxanthin synthase (encoded by the *crtS* gene) catalyzes the ketolation and hydroxylation of β-carotene to produce astaxanthin (Ojima et al. 2006). This enzyme is related to a member of the cytochrome P450 protein family and requires a redox partner for electron transfer, which for microsomal cytochrome P450s is generally a cytochrome P450 reductase (CPR; Alcaíno et al. 2012). In *X. dendrorhous*, the *crtR* gene encodes the yeast CPR, which is essential for the synthesis of astaxanthin (Alcaíno et al. 2008).

Among the mRNA levels of the genes controlling astaxanthin biosynthesis from β-carotene, the XR4 *crtS* gene transcript had the highest values, showing a continuous increase throughout cell growth (Fig. 2e). The transcript levels were 1.8- to 3.5-fold higher in XR4 than in the wild-type strain. According to the XR4 *crtS* sequence analysis, the only T–C transition in nucleotide 1256, corresponding to exon 7, does not cause an amino acid change in its protein sequence (Table 3). Miao et al. (2011) also reported a *crtS* mRNA increase during the growth phases of the overproducing carotenoid *X. dendrorhous* MK19 strain. Our results and those of others are in accordance with the fact that the single *crtS* gene product catalyzes the 4-ketolation and 3-hydroxylation of β-carotene to astaxanthin in *X. dendrorhous* (Ojima et al. 2006). Moreover, the low ratio of several astaxanthin precursors that are potential substrates of astaxanthin synthase, such as echinenone, canthaxanthin and phoenicoxanthin (Table 2; Visser et al. 2005) in the XR4 strain, is in accordance with its higher *crtS* transcript level that may increase astaxanthin synthase activity in this strain.

The *crtR* gene expression in XR4 was nearly twofold that observed in the wild-type strain in the early log phase and decreased throughout the growth curve, while carotenoid production increased (Fig. 2f). The *X. dendrorhous* astaxanthin-producing cytochrome P450 system is unique because astaxanthin synthase has a high specificity for its own CPR, encoded by *crtR* (Alcaíno et al. 2012). Ukibe et al. (2009) found that astaxanthin production was only achieved when *crtS* was coexpressed with *crtR* in a metabolically engineered *Saccharomyces cerevisiae* strain in which the *X. dendrorhous* carotenogenic genes were introduced. However, heterologous expression of several other cytochrome P450s in *S. cerevisiae* has been functionally successful, indicating that the endogenous *S. cerevisiae* CPR is capable of reducing a wide variety of P450s but not *X. dendrorhous* crtS (Ukibe et al. 2009).

Although astaxanthin synthase has a high specificity for its own CPR, we found no direct relationship between the mRNA level patterns from these genes. Other cytochrome P450s that have been described in *X. dendrorhous* include CYP51 (lanosterol 14-demethylase; Leiva et al. 2015) and CYP61 (C-22 sterol desaturase; Loto et al. 2012), which function in ergosterol biosynthesis and also could be related to *crtR*. As the *crtR* gene product should be acting as an electron donor for astaxanthin synthase as well as for other P450s, we can suggest, in agreement with other studies, the

existence of a different regulatory mechanism for *crtR* gene expression (Alcaíno et al. 2008; 2014).

As the regulation of the carotenoid pathway is not well understood in *X. dendrorhous*, the *crtR* XR4 sequence analysis could also help to partially explain our results. This gene showed the highest number of mutations (Table 3), with 60 nucleotide transitions and transversions in the promoter region that could affect the regulation of its expression, and 40 mutations associated with nucleotide changes in the ORF sequence.

Among the mutations found in the *crtR* promoter, four of them could be related to the decrease in the expression of this gene. The first two (G–A and A–G transitions found 831 and 833 nucleotides upstream of the translation initiation site, respectively) affected the sequence CAGGTA, located 829–834 nucleotides upstream of the translation initiation site. The sequence CAGGTA is considered as a binding site for the Mot3p nuclear transcription factor, which is involved in repression of ergosterol biosynthetic genes (Davies and Rine 2006). The last two mutations (A–T transversion and the G–A transition found 789 and 794 nucleotides upstream of the translation initiation site, respectively) affected the sequence TGAGTAA located 789–795 nucleotides upstream of the translation initiation site. This sequence is reported as a binding site for the Yap1p transcription factor, which is required for oxidative stress tolerance (Farrugia and Balzan 2012).

The mutations in the XR4 exonic regions resulted in a T residue insertion at position 37 (due to a CCA insertion after nucleotide 111, exon 1), the replacement of Y with D at position 52 (result of a T to G transversion of nucleotide 156, exon 1) and in the replacement of N with T at position 521 (due to an A insertion after nucleotide 1563, exon 3). The first two amino acid changes are located between the amino terminal transmembrane region and the conserved FMN-binding domain (the domain that interacts with P450 enzymes; Yadav and Loper 2000), whereas the third one is located between the FAD- and NAD(P)H-binding domains (Alcaíno et al. 2008, 2012). While the mutations did not affect the FMN, FAD or NAD(P)H-binding domains, the threonine hydroxyl group is fairly reactive and the short side chain of aspartate lends the amino acid a slightly stronger preference to be involved in protein-active sites (Betts and Russell 2007). This probably plays a role in the CrtR XR4 protein structure or stability, and could contribute to the carotenoid and astaxanthin-overproducing phenotype of the XR4 strain.

In general, increased formation of astaxanthin in mutant strains can be caused by a global up-regulation of the entire astaxanthin-synthesizing pathway or by overexpression of limiting enzymes in the specific pathway (Gassel et al. 2013). In the present study, not all of the carotenogenic structural genes showed high levels of their transcripts along the growth curve in the overproducing mutant; however, the results suggest that at least in part the higher *crtE* and *crtS* transcript levels can enhance the carotenoid pathway in the XR4 strain. While the *crtE* gene controls the first specific step of this pathway, allowing the isoprenoid precursors to flow toward the carotenogenic pathway, the *crtS* gene is directly involved in the formation of astaxanthin from β-carotene. The lack of an evident correlation between the mRNA levels of the carotenogenic genes and the synthesis of carotenoids has been previously reported (Lodato et al. 2007; Wozniak et al. 2011). According to these authors, our results also suggest that a possible explanation of the nonlinear relationship between carotenogenic transcript levels and carotenoid biosynthesis could be the fact that the necessary enzymes for carotenoid production are stable for a long time in the stationary phase of growth, making possible carotenoid synthesis.

Although the regulation of carotenoid biosynthesis is not completely elucidated in *X. dendrorhous*, the *crtYB*, *crtI* and *crtR* mutations identified in the XR4 genes, along with the high transcript levels of the *crtE* and *crtR* genes, could exert a positive regulatory effect on the entire carotenoid biosynthesis pathway of the mutant strain, thus allowing its higher astaxanthin and carotenoid production.

Carotenoid biosynthesis in *X. dendrorhous* is a complex process, which could be regulated at multiple levels, involving the concentration of carotenogenic gene mRNAs, the flow of metabolic intermediates among different pathways and perhaps also the level of the carotenogenic proteins and their enzymatic activities (Lodato et al. 2007). However, an integral analysis of growth, carotenoid production, carotenogenic genes transcriptional regulation and changes in gene sequences between a wild-type and a mutant *X. dendrorhous* strain elucidates the XR4 carotenoid-overproducing phenotype. Further research is necessary to continue elucidating the mechanisms involved in the genetic regulation and enzymatic activity involved in the carotenogenesis of *X. dendrorhous.*

Acknowledgments L. M. Castelblanco-Matiz and A. Barbachano-Torres thank Consejo Nacional de Ciencia y Tecnología, Mexico, for Ph.D. fellowships (219320 and 172824, respectively). This work was partially supported by Fondo Nacional de Desarrollo Científico y Tecnológico, Chile, Fondecyt 1140504.

References

Alcaíno J, Barahona S, Carmona M, Lozano C, Marcoleta A, Niklitschek M, Sepúlveda D, Baeza M (2008) Cloning of the cytochrome P450 reductase (*crtR*) gene and its involvement in the astaxanthin biosynthesis of *X. dendrhorhous*. BMC Microbiol 8:169. doi:10.1186/1471-2180-8-169

Alcaíno J, Fuentealba M, Cabrera R, Baeza M, Cifuentes V (2012) Modeling the interfacial interactions between CrtS and CrtR

from *Xanthophyllomyces dendrorhous*, a P450 system involved in astaxanthin production. J Agric Food Chem 60:8640–8647. doi:10.1021/jf302287f

Alcaíno J, Romero I, Niklitschek M, Sepúlveda D, Rojas MC, Baeza M, Cifuentes V (2014) Functional Characterization of the *Xanthophyllomyces dendrorhous* Farnesyl pyrophosphate synthase and geranylgeranyl pyrophosphate synthase encoding genes that are involved in the synthesis of isoprenoid precursors. PLoS One 9(5):e96626. doi:10.1371/journal.pone.0096626

Ambati RR, Phang SM, Ravi S, Aswathanarayana RG (2014) Astaxanthin: sources, extraction, stability, biological activities and its commercial applications—a review. Mar Drugs 12:128–152. doi:10.3390/md12010128

An GH, Schuman DB, Johnson EA (1989) Isolation of *Phaffia rhodozyma* mutants with increased astaxanthin content. Appl Environ Microbiol 55:116–124

Barbachano-Torres A, Castelblanco-Matiz LM, Ramos-Valdivia AC, Cerda-García-Rojas CM, Salgado-Rodríguez LM, Flores-Ortiz C, Ponce-Noyola T (2014) Analysis of proteomic changes in colored mutants of *Xanthophyllomyces dendrorhous* (*Phaffia rhodozyma*). Arch Microbiol 196:411–421. doi:10.1007/s00203-014-0979-x

Betts MJ, Russell RB (2007) Amino-acid properties and consequences of substitutions. In: Barnes MR (ed) Bioinformatics for geneticists: a bioinformatics primer for the analysis of genetic data, 2nd edn. Wiley, New Jersey, pp 311–342. doi:10.1002/0470867302.ch14

Boyle JS, Lew AM (1995) An inexpensive alternative to glassmilk for DNA purification. Trends Genet 11:8

Breitenbach J, Visser H, Verdoes JC, van Ooyen AJJ, Sandmann G (2011) Engineering of geranylgeranyl pyrophosphate synthase levels and physiological conditions for enhanced carotenoid and astaxanthin synthesis in *Xanthophyllomyces dendrorhous*. Biotechnol Lett 33:755–761. doi:10.1007/s10529-010-0495-2

Britton G, Liaaen-Jensen S, Pfander H (2008) Carotenoids handbook. Birkhäuser Verlag, Switzerland

Chávez-Cabrera C, Flores-Bustamante ZR, Marsch R, Montes MC, Sánchez S, Cancino-Díaz JC, Flores-Cotera LB (2010) ATP-citrate lyase activity and carotenoid production in batch cultures of *Phaffia rhodozyma* under nitrogen-limited and nonlimited conditions. Appl Microbiol Biotechnol 85:1953–1960. doi:10.1007/s00253-009-2271-6

Chimsung N, Tantikitti C, Milley JE, Verlhac-Trichet V, Lall SP (2014) Effects of various dietary factors on astaxanthin absorption in Atlantic salmon (*Salmo salar*). Aquac Res 45:1611–1620. doi:10.1111/are.12108

Chomczynski P, Sacchi N (1987) Single-step method of RNA isolation by acid guanidinium thiocyanate-phenol-chloroform extraction. Anal Biochem 162:156–159. doi:10.1016/0003-2697(87)90021-2

Davies BSJ, Rine J (2006) A role for sterol levels in oxygen sensing in *Saccharomyces cerevisiae*. Genetics 174:191–201. doi:10.1534/genetics.106.059964

Farrugia G, Balzan R (2012) Oxidative stress and programmed cell death in yeast. Front Oncol 2:1–21. doi:10.3389/fonc.2012.00064

Gassel S, Schewe H, Schmidt I, Schrader J, Sandmann G (2013) Multiple improvement of astaxanthin biosynthesis in *Xanthophyllomyces dendrorhous* by a combination of conventional mutagenesis and metabolic pathway engineering. Biotechnol Lett 35:565–569. doi:10.1007/s10529-012-1103-4

Gassel S, Breitenbach J, Sandmann G (2014) Genetic engineering of the complete carotenoid pathway towards enhanced astaxanthin formation in *Xanthophyllomyces dendrorhous* starting from a high-yield mutant. Appl Microbiol Biotechnol 98:345–350. doi:10.1007/s00253-013-5358-z

Leiva K, Werner N, Sepúlveda D, Barahona S, Baeza M, Cifuentes V, Alcaíno J (2015) Identification and functional characterization of the *CYP51* gene from the yeast *Xanthophyllomyces dendrorhous* that is involved in ergosterol biosynthesis. BMC Microbiol 15:89. doi:10.1186/s12866-015-0428-2

Lodato P, Alcaino J, Barahona S, Retamales P, Jimenez A, Cifuentes V (2004) Study of the expression of carotenoid biosynthesis genes in wild-type and deregulated strains of *Xanthophyllomyces dendrorhous* (*Ex.: Phaffia rhodozyma*). Biol Res 37:83–94

Lodato P, Alcaíno J, Barahona S, Niklitschek M, Carmona M, Wozniak A, Baeza M, Jiménez A, Cifuentes V (2007) Expression of the carotenoid biosynthesis genes in *Xanthophyllomyces dendrorhous*. Biol Res 40:73–84. doi:10.4067/S0716-97602007000100008

Loto I, Gutiérrez MS, Barahona S, Sepúlveda D, Martínez-Moya P, Baeza M, Cifuentes V, Alcaíno J (2012) Enhancement of carotenoid production by disrupting the C22-sterol desaturase gene (CYP61) in *Xanthophyllomyces dendrorhous*. BMC Microbiol 12:235–251

Marcoleta A, Niklitschek Wozniak A, Lozano C, Alcaíno J, Baeza M, Cifuentes V (2011) Glucose and ethanol-dependent transcriptional regulation of the astaxanthin biosynthesis pathway in *Xanthophyllomyces dendrorhous*. BMC Microbiol 11:190–201. doi:10.1186/1471-2180-11-190

Miao L, Chi S, Tang Y, Su Z, Yin T, Guan G, Li Y (2011) Astaxanthin biosynthesis is enhanced by high carotenogenic gene expression and decrease of fatty acids and ergosterol in a *Phaffia rhodozyma* mutant strain. FEMS Yeast Res 11:192–201. doi:10.1111/j.1567-1364.2010.00705.x

Ojima K, Breitenbach J, Visser H, Setoguchi Y, Tabata K, Hoshino T, van den Berg J, Sandmann G (2006) Cloning of the astaxanthin synthase gene from *Xanthophyllomyces dendrorhous* (*Phaffia rhodozyma*) and its assignment as a β-carotene 3-hydroxylase/4-ketolase. Mol Genet Genomics 275:148–158. doi:10.1007/s00438-005-0072-x

Rintala E, Toivari M, Pitkänen JP, Wiebe MG, Ruohonen L, Penttilä M (2009) Low oxygen levels as a trigger for enhancement of respiratory metabolism in *Saccharomyces cerevisiae*. BMC Genom 10:461–480. doi:10.1186/1471-2164-10-461

Rodriguez-Saiz M, de la Fuente JL, Barredo JL (2010) *Xanthophyllomyces dendrorhous* for the industrial production of astaxanthin. Appl Microbiol Biotechnol 88:645–658. doi:10.1007/s00253-010-2814-x

Rolland F, Winderickx J, Thevelein JM (2002) Glucose-sensing and -signalling mechanisms in yeast. FEMS Yeast Res 2:183–201

Sambrook J, Russell DW (2001) Molecular cloning a laboratory manual, 3rd edn. Cold Spring Harbor, New York

Schmidt I, Schewe H, Gassel S, Jin C, Buckingham J, Hümbelin M, Sandmann G, Schrader J (2011) Biotechnological production of astaxanthin with *Phaffia rhodozyma/Xanthophyllomyces dendrorhous*. Appl Microbiol Biotechnol 89:555–571. doi:10.1007/s00253-010-2976-6

Schmittgen TD, Livak KJ (2008) Analyzing real-time PCR data by the comparative C_T method. Nat Protoc 3:1101–1108. doi:10.1038/nprot.2008.73

Schroeder WA, Johnson EA (1995) Singlet oxygen and peroxyl radicals regulate carotenoid biosynthesis in *Phaffia rhodozyma*. J Biol Chem 270:18374–18379

Teixeira MC, Monteiro PT, Guerreiro JF, Gonçalves JP, Mira NP, dos Santos SC, Cabrito TR, Palma M, Costa C, Francisco AP, Madeira SC, Oliveira AL, Freitas AT, Sá-Correia I (2014) The YEASTRACT database: an upgraded information system for the analysis of gene and genomic transcription regulation in *Saccharomyces cerevisiae*. Nucl Acids Res 42:161–166. doi:10.1093/nar/gkt1015

Ukibe K, Hashida K, Yoshida N, Takagi H (2009) Metabolic engineering of *Saccharomyces cerevisiae* for astaxanthin production and oxidative stress tolerance. Appl Environ Microbiol 75:7205–7211. doi:10.1128/AEM.01249-09

Verdoes JC, Misawa N, van Ooyen AJJ (1999) Cloning and characterization of the astaxanthin biosynthetic gene encoding phytoene desaturase of *Xanthophyllomyces dendrorhous*. Biotechnol Bioeng 63:750–755

Verdoes JC, Sandmann G, Visser H, Diaz M, van Mossel M, van Ooyen AJJ (2003) Metabolic engineering of the carotenoid biosynthetic pathway in the yeast *Xanthophyllomyces dendrorhous* (*Phaffia rhodozyma*). Appl Environ Microbiol 69:3728–3738. doi:10.1128/AEM.69.7.3728-3738.2003

Visser H, van Ooyen AJJ, Verdoes JC (2003) Metabolic engineering of the astaxanthin-biosynthetic pathway of *Xanthophyllomyces dendrorhous*. Yeast Res 4:221–231. doi:10.1016/S1567-1356(03)00158-2

Visser H, Sandmann G, Verdoes JC (2005) Xanthophylls in fungi: metabolic engineering of the astaxanthin biosynthetic pathway in *Xantophyllomyces dendrorhous*. In: Barredo JL (ed) Methods in biotechnology: microbial processes and products, 1st edn. Humana, Totowa NJ, pp 257–272

Wozniak A, Lozano C, Barahona S, Niklitschek M, Marcoleta A, Alcaíno J, Sepulveda D, Baeza M, Cifuentes V (2011) Differential carotenoid production and gene expression in *Xanthophyllomyces dendrorhous* grown in a non-fermentable carbon source. FEMS Yeast Res 11:252–262. doi:10.1111/j.1567-1364.2010.00711.x

Yadav JS, Loper JC (2000) Cytochrome P450 oxidoreductase gene and its differentially terminated cDNAs from the white rot fungus *Phanerochaete chrysosporium*. Curr Genet 37:65–73